AIP | Applied Physics Letters

Thermal conductivity of ultrathin nano-crystalline diamond films determined by Raman thermography assisted by silicon nanowires

Julian Anaya, Stefano Rossi, Mohammed Alomari, Erhard Kohn, Lajos Tóth, Béla Pécz, and Martin Kuball

Citation: Applied Physics Letters **106**, 223101 (2015); doi: 10.1063/1.4922035
View online: http://dx.doi.org/10.1063/1.4922035
View Table of Contents: http://scitation.aip.org/content/aip/journal/apl/106/22?ver=pdfcov
Published by the AIP Publishing

Thermal conductivity of ultrathin nano-crystalline diamond films determined by Raman thermography assisted by silicon nanowires

Julian Anaya,[1] Stefano Rossi,[2] Mohammed Alomari,[2] Erhard Kohn,[2] Lajos Tóth,[3] Béla Pécz,[3] and Martin Kuball[1]
[1]*Center for Device Thermography and Reliability, University of Bristol, Bristol BS8 1TL, United Kingdom*
[2]*Institute of Electron Devices and Circuits (EBS), Ulm University, Ulm 89081, Germany*
[3]*Thin Film Physics Department, Institute for Technical Physics and Materials Science, Budapest H-1525, Hungary*

(Received 18 February 2015; accepted 21 May 2015; published online 1 June 2015)

The thermal transport in polycrystalline diamond films near its nucleation region is still not well understood. Here, a steady-state technique to determine the thermal transport within the nano-crystalline diamond present at their nucleation site has been demonstrated. Taking advantage of silicon nanowires as surface temperature nano-sensors, and using Raman Thermography, the in-plane and cross-plane components of the thermal conductivity of ultra-thin diamond layers and their thermal barrier to the Si substrate were determined. Both components of the thermal conductivity of the nano-crystalline diamond were found to be well below the values of polycrystalline bulk diamond, with a cross-plane thermal conductivity larger than the in-plane thermal conductivity. Also a depth dependence of the lateral thermal conductivity through the diamond layer was determined. The results impact the design and integration of diamond for thermal management of AlGaN/GaN high power transistors and also show the usefulness of the nanowires as accurate nano-thermometers. © *2015 AIP Publishing LLC*. [http://dx.doi.org/10.1063/1.4922035]

Diamond with its high thermal conductivity (κ)[1,2] has an outstanding potential for enhancing the thermal management of electronic devices.[3–6] To take full advantage of it, the diamond should be used as close as possible to the heat source, for example, to the electron channel in an AlGaN/GaN high electron mobility transistor (HEMT).[5–10] Managing efficiently the Joule self-heating in these devices is essential for increasing achievable electrical power densities and for improving the device operational lifetime,[11] making therefore their integration with diamond very attractive. Rather than using the diamond only as a heat spreader attached to the semiconductor device chip, different proposals have emerged recently for growing polycrystalline diamond directly onto different parts of AlGaN/GaN HEMTs for heat sinking.[3–11] This strategies typically rely on replacing the Si or SiC substrate,[3,7] and/or growing the diamond on top of the HEMT channel,[8–10,12,13] which ultimately means that the heat flux has to diffuse across the nucleation region of the polycrystalline diamond, in which the size of the crystals lies in the nanoscale.[14] Polycrystalline diamond can reach κ values similar to those from single crystal diamond (>2000 W/mK).[15] However, it is known that the abundance of grain boundaries, and therefore, the grain size, can reduce dramatically its thermal conductivity.[16–18] The average distance phonons travel between scattering events (MFP) in the bulk diamond lattice is very large, being ~80% of the heat carried by phonons with MFPs greater than 200 nm at room temperature,[19] making the role of the grain boundaries especially critical near the nucleation region. Here, the lateral dimensions of the grains, which typically develop in a columnar shape, are not greater than a few hundreds of nanometers.[14] To determine the thermal characteristics in the near nucleation region, measuring the κ of ultra-thin layers of columnar nano-crystalline diamond (c-NCD) is needed; however, this is a challenging task, which is mostly performed with transient measurements.[20–25] Nevertheless, these transient techniques are indirect methods having access only to the thermal diffusivity, which requires a complex data analysis for extracting the thermal conductivity. As a result, in-plane thermal conductivities ranging from 20 W/mK (Refs. 20 and 25) to 500 W/mK (Ref. 26) and cross-plane thermal conductivities ranging from 80 W/mK (Ref. 24) to more than 800 W/mK (Refs. 22, 26, and 27) have been reported for sub 2 μm c-NCD.[22,26] These large variations in the reported values of κ may arise not only from differences in the samples but also because of the different experimental techniques used in each experiment.[28] This makes it difficult to draw a clear conclusion about the phonon transport near the polycrystalline diamond nucleation site, i.e., in the c-NCD region. Therefore, despite being a crucial factor for the optimal design of the next generation HEMTs with high dissipation capability, extremely little is known about the thermal properties of diamond near the nucleation site.

In this letter, a steady-state approach for measuring the key thermal parameters of polycrystalline diamond near the nucleation site is reported. The technique relies only on one direct measurement technique, Raman thermography, making use of silicon nanowires (NWs) acting as accurate surface nano-thermometers. This enables the extraction of both the in-plane and the cross-plane κ as well as the thermal resistance between the diamond and the substrate.

The study has been carried out on polycrystalline diamond films nucleated by bias enhance nucleation (BEN) on 275 μm thick single crystalline Si ⟨100⟩ wafers, grown by hot filament chemical vapor deposition (CVD) at 750 °C and 1.5 kPa, with 0.4% CH_4 diluted in H_2. Under such deposition conditions, the resulting diamond film has a columnar nanostructure (c-NCD),[14] with elongated grains along the out-of-

plane direction (i.e., normal to the substrate). In this condition, samples with different thicknesses (1 μm and 680 nm) were grown stepwise. To enable controlled heating of the diamond for the determination of the thermal conductivity, gold metal heaters, 100 nm thick and 5 μm wide were deposited onto the diamond film surface, including a 10 nm thick titanium adhesion layer. Current and voltage were independently measured in a 4-probe configuration for an accurate control of the Joule heating dissipated in the metal heater structure.

For measuring the in-plane thermal conductivity, thin membranes, as shown in Fig. 1(a), were used with a $\sim$100 $\times$ 500 μm area, after etching away the silicon below the diamond. This results in a wide area at the center of the membrane, in which the heat flow is linear from the metal heater laterally through the diamond membrane. For analyzing the cross-plane thermal conductivity, ring heaters were fabricated on the same wafers (see Fig. 1(b)). This annular structure creates a radial symmetric temperature field, which keeps the heater in a near-isothermal region, ensuring a homogenous power dissipation in the heater. The diamond is also etched away outside the heater, thus minimizing the radial (in-plane) heat spreading inside the diamond membrane by geometrical confinement, thus, increasing the role of the cross-plane heat transport across the c-NCD. For measuring temperatures, Raman thermography was used in the fabricated structures, this has been successfully tested for similar purposes elsewhere.[6,30–33] A Renishaw InVia Raman system with a Raman shift resolution better than 0.1 cm^{-1} was employed, using a 488 nm Ar-ion laser line focused with an 0.65 N.A. 50$\times$ objective onto a spot size smaller than 1 μm.[6] The temperature dependence of the phonon mode of diamond was determined for the studied layers by heating the films in a hot stage (see Fig. 1(c)). This increased the accuracy since the residual stress in the grains impacts some degree to the temperature dependence of the phonons in the c-NCD. A typical Raman spectrum of the c-NCD films under study is shown in the inset of Fig. 1(c). Note the distinct sp^3 diamond peak (1332.3 cm^{-1}) in the spectrum and the absence of peaks near 1100 cm^{-1} and 1500–1600 cm^{-1} corresponding to graphitic and non-sp^3 phases features, which are typically identified in low thermal conductivity polycrystalline diamond.[34,35] However, near the nucleation interface some non-diamond phases appears in the first tens of nanometers (Fig. 1(d)). Since diamond is transparent for the laser wavelength used here, the whole thickness of the diamond membrane is measured, and it is also possible to simultaneously measure the temperature of the Si substrate, with the signal originating from the first $\sim$0.5 μm of the Si due to the absorption of the laser within the Si, thus enabling the measurement of the ΔT between the NCD and the Si.

Silicon (Si) NW—$\sim$50 nm in diameter and 2–5 μm in length—similar to those described in Ref. 36 were deposited onto the metal heaters and onto the diamond surface (see Fig. 2(a)). The purpose of the Si NWs is to act as accurate local nano-thermometers through its phonon frequency temperature dependence, which has a similar linear behavior than the bulk Si (0.0222 cm^{-1}/K (NWs) vs 0.0224 cm^{-1}/K (bulk Si), Fig. 2(b)). Since the Si NWs can absorb energy from the laser, care needs to be taken to avoid sizable self-heating effect in the NWs.[36] However, it has been recently demonstrated that the Raman signal of Si NWs can be collected using ultralow laser powers, typically, $<$10 μW (see Fig. 2(c)), removing any self-heating effect.[36] This is possible due to an electromagnetic coupling between the laser beam and the leaky modes of the NWs on some substrates such as Au.[37–39] Here, the electric field inside the NWs is enhanced, which ultimately results in a great increase of the Raman signal due to its dependence with $|E|^2$.[37–39]

The NWs small dimension minimizes the heat transfer with low density media, such as air, resulting in a near perfectly thermal isolation of the Si NWs from the surrounding air.[36,40] This, combined with their small mass, leads to a good thermalization with the surface in direct contact with the Si NWs.[36,40] All of these properties make the Si NWs therefore excellent Raman nanosensors, allowing to extract

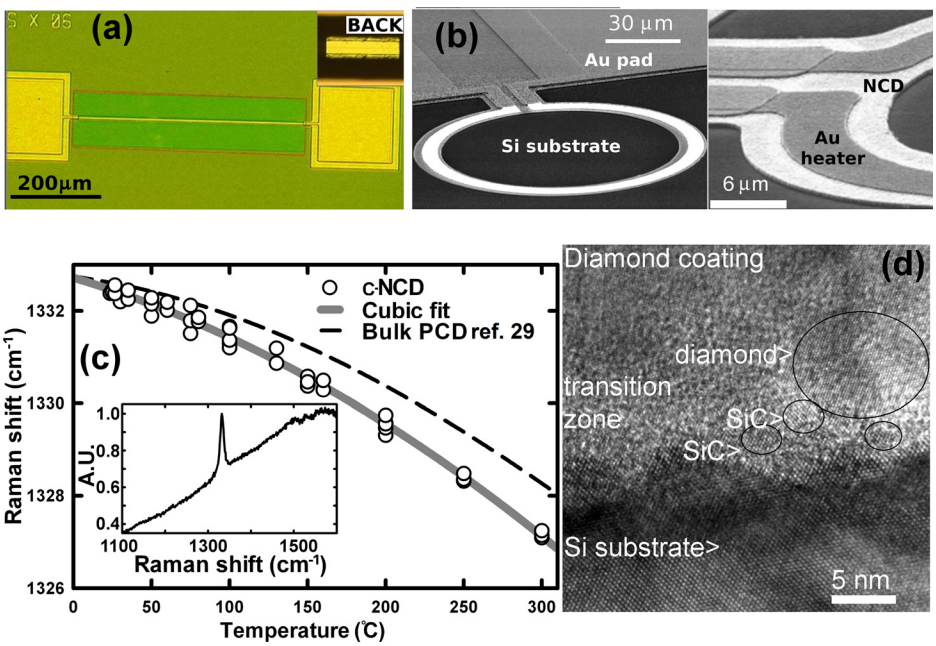

FIG. 1. (a) Optical micrograph and (b) Electron microscopy (SEM) of the test structures used for analyzing the heat transport in c-NCD diamond. (c) Temperature dependence of the c-NCD diamond Raman shift. Inset displays typical Raman spectrum collected from the c-NCD samples used in this work.[29] (d) High resolution transmission electron microscopy micrograph of the 1 μm NCD sample at the nucleation interface. Note the existence of a transition zone containing various nano-crystalline grains and amorphous/metastable phases.

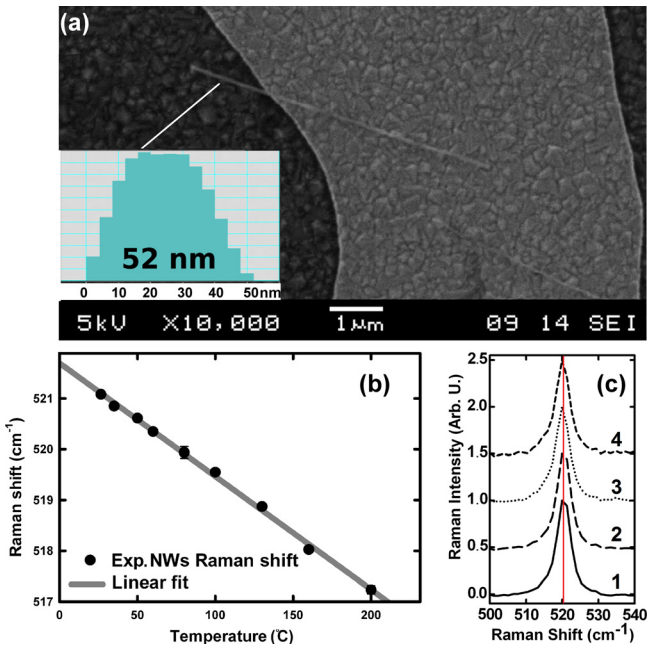

FIG. 2. (a) SEM micrograph Si NWs (5 μm length, 53 nm in diameter) deposited onto the metal heaters. (b) Temperature dependence of the Raman shift of individual Si NWs deposited onto the heaters. (c) Raman shift of a NW for a set of four increasing powers, ~5 μW (1), ~10 μW (2), 25 μW (3), and ~50 μW (4).

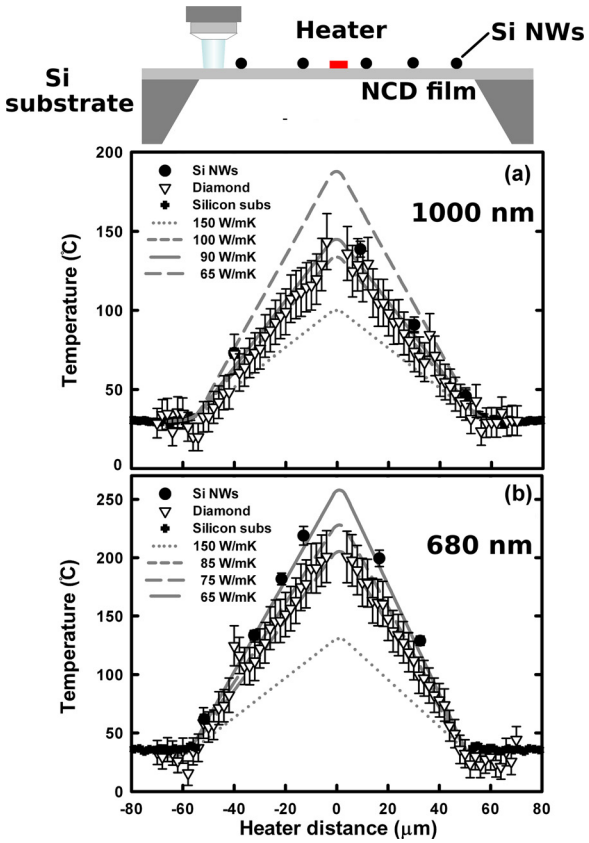

FIG. 3. Temperature profiles measured in the c-NCD membranes with the line heater positioned in the center. Lines correspond to temperatures obtained from fitting the numerical model (ANSYS) to the experimental data using the indicated thermal conductivities.

the temperature of non-Raman active materials such as the metals of the here studied structures with high spatial resolution.

Temperature profiles obtained on the diamond membranes (as in Fig. 1(a)) are shown in Fig. 3, for diamond films of 1 μm and 680 nm thickness (Figs. 3(a) and 3(b), respectively) when an electrical power of 0.2 W is dissipated in the metal heater. Peak temperature is located, where the metal heater is deposited, and it decreases along the membrane away from the metal heater. Small deviations from a linear behavior of the temperature profile are observed when temperatures are determined from the diamond Raman modes alone, in particular, near the location of the metal line heater. This is most likely due to stress contributions to the Raman peak position. For a stress-free measurement, Si NWs aligned parallel to the line heater were used as surface nano-thermometers, resulting in a significant improvement of the accuracy of the measurement of the temperature profiles.

The thermal conductivity of the diamond films was extracted by fitting the measured temperature profiles to a numerical solution of the heat equation on the exact three dimensional (3D) finite element model in each case (Fig. 3, lines). The temperature dependence of the silicon substrate κ,[41] and losses by radiation and natural convection were taken into account in the model. The fitted value for κ was nearly independent of the power dissipated in the structure (peak temperature in the heater from 100 up to 400 °C). This illustrates that for this temperature range, κ is nearly constant. This is consistent with what is expected for c-NCD.[18] Using this approach, κ values of 65 ± 5 W/mK and 95 ± 5 W/mK for the 680 nm and 1 μm membranes were determined, respectively. These figures are in good agreement with those reported in Ref. 20 for similar c-NCD thin layers, for which, however, no cross-plane thermal conductivity values were reported. Given that the two samples were grown under the same conditions, the only difference between the two samples lies in their average lateral grain size; the grains of the thicker samples when measured from the top surface are a ~25% larger than the ones for the thinner sample (160 nm vs 130 nm). This will impact the in-plane κ through phonon grain boundary scattering,[16–18] explaining why the sample with the smaller average grains has a smaller in-plane κ. However, being the two samples grown stepwise in identical conditions, their initial grain evolution should be identical. Therefore, the 1 μm thick sample was considered using a two layer model with a bottom layer of 680 nm (65 W/mK), and allowing the κ of the top 320 nm layer to be a free fitting parameter. Using this approach, an in-plane κ of 150 W/mK for the top 320 nm was found to fit the experimental temperature profile measured in the 1 μm sample. Therefore, the lateral expansion of the columnar grains results in a depth-dependence of the in-plane κ in the c-NCD layer. This result impact the optimal integration of the c-NCD on top of a HEMT channel, in which the in-plane κ for a given thickness of the diamond film should be maximized by engineering the c-NCD grain evolution.

For the cross-plane thermal transport, we focus on the 1 μm thick c-NCD film which was explored by means of the ring structures, as shown in Fig. 1(b). Again Si NWs were deposited in this case onto the metal heater surface for

measuring the local temperature in the metal (see Fig. 2(a)). The temperature versus the electrical power dissipated in the heater was determined for the diamond and the Si substrate at symmetric points at a distance of ~500 nm from the heater (see Fig. 4 sketch, points A and B). Heater temperature was also determined from the Si NWs deposited onto the metal near points A and B. Knowing the lateral thermal conductivity of the c-NCD (95 W/mK) and solving the heat equation numerically in the exact 3D finite element model, a total thermal resistance of 55.5 ± 1.5 m^2K/GW between the metal and the substrate was determined from the silicon substrate and silicon NWs temperature profiles. If this thermal resistance is entirely attributed to the c-NCD, it corresponds to a thermal conductivity of ~18 W/mK—κ = thickness/thermal resistance. However, this rather low cross-plane κ also includes the contributions of the two thermal boundary resistances (TBRs): Ti/c-NCD and c-NCD/Si substrate. When the c-NCD temperature profile and the known TBR value for the Ti/diamond interface—9.5 ± 0.5 m^2K/GW from room temperature and above—[42] are included, it is possible to unambiguously determine the different contributions to the vertical thermal resistance of the c-NCD layer. The simultaneous fitting of all the measured temperature points in the test structure (Fig. 4) leads to a c-NCD/Si TBR of 42.2 ± 1.0 m^2K/GW, and a c-NCD vertical thermal resistance of 3.3 ± 1.3 m^2K/GW. This corresponds to a cross-plane κ of ~300 W/mK for the 1 μm thick diamond film. Using the same strategy, a vertical thermal resistance for the 680 nm thick c-NCD film of 2.7 ± 1.0 m^2K/GW, corresponding to a cross-plane κ of ~250 W/mK, was extracted (inset of Fig. 4). This values are in the ranges reported by other authors for c-NCD layers of similar thicknesses (~180–500 W/mK),[21–23] while the diamond/substrate TBR is similar to the one reported in Ref. 24 for c-NCD on Si. Combining these results with the ones obtained for the in-plane κ leads to an anisotropy ratio of ~3 for the in-plane/cross-plane κ, thus higher than the ~50% observed in bulk polycrystalline diamond.[43] However, the accuracy of the determination of the cross-plane conductivity of the diamond is limited by the dominant role played by the TBR between the c-NCD and the silicon. Its contribution is approximately one order of magnitude larger than the c-NCD contribution to the total cross-plane thermal resistance. Considering that in the diffuse-mismatch model, the phonon rejection for the silicon/diamond interface only accounts for roughly 5 m^2K/GW,[44] most of the thermal resistance should be addressed to the c-NCD region in direct contact with the substrate. This region is shown with more detail in Fig. 1(d), being clear the existence of a rough transition zone of 5–25 nm composed of very small diamond nanocrystals and cubic phase SiC particles embedded in an amorphous matrix. This defective transition region in the c-NCD acts as a bottleneck for the cross-plane thermal transport, being crucial the optimization of this region for taking full advantage of the polycrystalline diamond as an efficient substrate for HEMTs.[45]

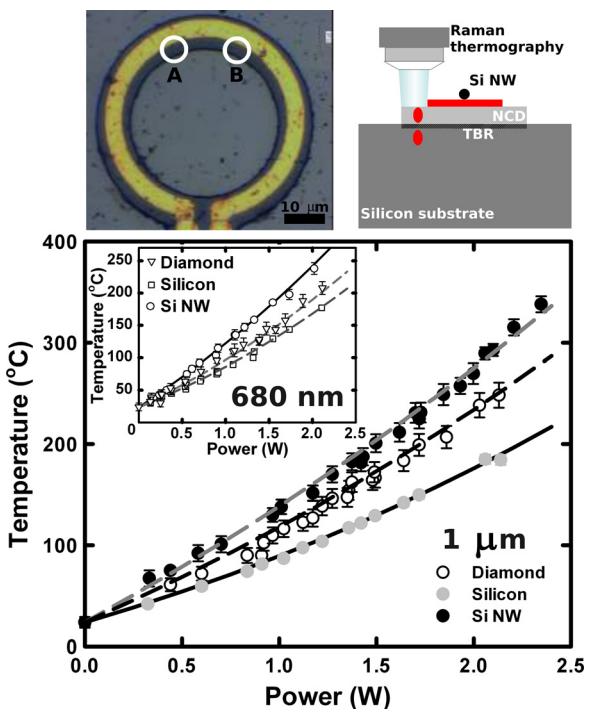

FIG. 4. Temperature as function of electrical power measured in the ring structures, as illustrated in the top of the figure, in the diamond, the Si, and on top of the metal heaters (NWs). The lines show the results from the simultaneous fitting in the numerical model when a c-NCD/Si TBR of 42.2 m^2K/GW and a c-NCD vertical thermal resistance of 3.3 m^2K/GW is assumed.

In conclusion, taking advantage of Si NWs and standard Raman Thermography, a steady-state method for extracting the thermal parameters of ultrathin diamond films has been developed. The in-plane and cross-plane components of the thermal conductivity as well as the thermal barrier in the diamond/substrate interface have been measured with this technique. We found a strong depth-dependence of the lateral κ induced by the grain evolution during the c-NCD growing process. Also a higher cross-plane than in-plane thermal conductivity has been found in the samples resulting in an anisotropic heat transport in the polycrystalline diamond thin layers. However, the cross-plane thermal transport seems to be dominated by the first nanometers near the nucleation interface. These results contributes to gain insight in the near nucleation heat transport of polycrystalline diamond, and are specially relevant for the integration of diamond near the electron channel in AlGaN/GaN devices, in which the special characteristics of the polycrystalline diamond thermal conductivity in the first micron cannot be neglected.

We acknowledge the financial support from ONR Global under the Award No.: N62909-13-1-N210. B.P. and L.T. also thank the support of the OTKA (Hungary) Grant No. K108869. We want to thank T. Rodriguez and A. Rodriguez from Universidad Politécnica de Madrid for providing the Si NWs used in this work.

[1]G. Slack, J. Phys. Chem. Solids **34**, 321 (1973).
[2]T. R. Anthony, W. F. Banholzer, J. F. Fleischer, L. Wei, P. K. Kuo, R. L. Thomas, and R. W. Pryor, Phys. Rev. B **42**, 1104 (1990).
[3]J. G. Felbinger, M. V. S. Chandra, Y. Sun, L. F. Eastman, J. Wasserbauer, F. Faili, D. Babic, D. Francis, and F. Ejeckam, IEEE Electron Device Lett. **28**, 11 (2007).
[4]M. Alomari, A. Dussaigne, D. Martin, N. Grandjean, C. Gaquiere, and E. Kohn, Electron. Lett. **46**, 299 (2010).
[5]Q. Diduck, J. Felbinger, L. F. Eastman, D. Francis, J. Wasserbauer, F. Faili, D. I. Babić, and F. Ejeckam, Electron. Lett. **45**, 758 (2009).

[6]J. W. Pomeroy, M. Bernardoni, D. C. Dumka, D. M. Fanning, and M. Kuball, Appl. Phys. Lett. **104**, 083513 (2014).
[7]J. Cho, Z. Li, E. Bozorg-Grayeli, T. I. Kodama, D. Francis, F. Ejeckam, F. Faili, M. Asheghi, and K. E. Goodson, IEEE Trans. Compon. Packag. Manuf. Technol. **3**, 79 (2013).
[8]M. J. Tadjer, T. J. Anderson, K. D. Hobart, T. I. Feygelson, J. D. Caldwell, C. R. Eddy, Jr., F. J. Kub, J. E. Butler, B. Pate, and J. Melngailis, IEEE Electron Device Lett. **33**, 23 (2012).
[9]M. Seelmann-Eggebert, P. Meisena, F. Schaudela, P. Koidla, A. Vescanb, and H. Leier, Diamond Relat. Mater. **10**, 744 (2001).
[10]T. J. Anderson, A. D. Koehler, K. D. Hobart, M. J. Tadjer, T. I. Feygelson, J. K. Hite, B. B. Pate, F. J. Kub, and C. R. Eddy, Jr., IEEE Electron Device Lett. **34**, 1382 (2013).
[11]S. M. Lee, R. Vetury, J. D. Brown, S. R. Gibb, W. Z. Cai, J. M. Sun, D. S. Green, and J. Shealy, in *Proceedings of the 46th Annual International Reliability Physics Symposium, Phoenix, USA* (2008), pp. 446–449.
[12]A. Wang, M. J. Tadjer, and F. Calle, Semicond. Sci. Technol. **28**, 055010 (2013).
[13]M. Alomari, M. Dipalo, S. Rossi, M. A. Diforte-Poisson, S. Delage, J.-F. Carlin, N. Grandjean, C. Gaquiere, L. Toth, B. Pecz, and E. Kohn, Diamond Relat. Mater. **20**, 604 (2011).
[14]O. A. Williams, Diamond Relat. Mater. **20**, 621 (2011).
[15]J. E. Graebner, M. E. Reiss, L. Seibles, T. M. Hartnett, R. P. Miller, and C. J. Robinson, Phys. Rev. B **50**, 3702 (1994).
[16]M. A. Angadi, T. Watanabe, A. Bodapati, X. Xiao, O. Auciello, J. A. Carlisle, J. A. Eastman, P. Keblinski, P. K. Schelling, and S. R. Phillpot, J. Appl. Phys. **99**, 114301 (2006).
[17]J. E. Graebner, S. Jin, G. W. Kammlott, J. A. Herb, and C. F. Gardinier, Appl. Phys. Lett. **60**, 1576 (1992).
[18]W. L. Liu, M. Shamsa, I. Calizo, A. A. Balandin, V. Ralchenko, A. Popovich, and A. Saveliev, Appl. Phys. Lett. **89**, 171915 (2006).
[19]W. Li, N. Mingo, L. Lindsay, D. A. Broido, D. A. Stewart, and N. A. Katcho, Phys. Rev. B **85**, 195436 (2012).
[20]K. Plamann, D. Fournier, E. Anger, and A. Gicquel, Diamond Relat. Mater. **3**, 752 (1994).
[21]H. Verhoeven, A. Flöter, H. Reiß, R. Zachai, D. Wittorf, and W. Jäger, Appl. Phys. Lett. **71**, 1329 (1997).
[22]J. Philip, P. Hess, T. Feygelson, J. E. Butler, S. Chattopadhyay, K. H. Chen, and L. C. Chen, J. Appl. Phys. **93**, 2164 (2003).
[23]A. Sood, J. Cho, K. D. Hobart, T. Feygelson, B. Pate, M. Asheghi, and K. E. Goodson, in *14th IEEE ITHERM Conference* (2014), p. 1192.
[24]K. E. Goodson, O. W. Käding, M. Rösler, and R. Zachai, J. Appl. Phys. **77**(4), 1385 (1995).
[25]B. Lee, J. S. Lee, S. U. Kim, K. Kim, O. Kwon, S. Lee, J. H. Kim, and D. S. Lim, J. Vac. Sci. Technol., B **27**, 2408 (2009).
[26]S. Rossi, M. Alomari, Y. Zhang, S. Bychikhin, D. Pogany, J. M. R. Weaver, and E. Kohn, Diamond Relat. Mater. **40**, 69–74 (2013).
[27]E. Bozorg-Grayeli, A. Sood, M. Asheghi, V. Gambin, R. Sandhu, T. I. Feygelson, B. B. Pate, K. Hobart, and K. E. Goodson, Appl. Phys. Lett. **102**, 111907 (2013).
[28]J. E. Graebner, H. Altmann, N. M. alzaretti, R. Campbell, H.-B. Chae, A. Degiovanni, R. Enck, A. Feldman, D. Fournier, J. Fricke, J. S. Goela, K. J. Gray, Y. Q. Gu, I. Hatta, T. M. Hartnett, R. E. Imhof, R. Kato, P. Koidl, P. K. Kuo, T.-K. Lee, D. Maillet *et al.*, Diamond Relat. Mater. **7**, 1589 (1998).
[29]J. B. Cui, K. Amtmann, J. Ristein, and L. Ley, J. Appl. Phys. **83**, 7929 (1998).
[30]S. Perichon, V. Lysenko, B. Remaki, D. Barbier, and B. Champagnon, J. Appl. Phys. **86**, 4700 (1999).
[31]A. Jungen, C. Stampfer, and C. Hierold, Appl. Phys. Lett. **88**, 191901 (2006).
[32]G. S. Doerk, C. Carraro, and R. Maboudian, ACS Nano **4**(8), 4908 (2010).
[33]J. S. Reparaz, E. Chavez-Angel, M. R. Wagner, B. Graczykowski, J. Gomis-Bresco, F. Alzina, and C. M. Sotomayor Torres, Rev. Sci. Instrum. **85**, 034901 (2014).
[34]A. Ono, T. Baba, H. Funamoto, and A. Nishikawa, Jpn. J. Appl. Phys., Part 2 **25**, L808 (1986).
[35]E. Wörner, J. Wagner, W. MüllerSebert, C. Wild, and P. Koidl, App. Phys. Lett. **68**, 1482 (1996).
[36]J. Anaya, A. Torres, V. Hortelano, A. C. Prieto, A. Rodríguez, T. Rodriguez, and J. Jiménez, App. Phys. A **114**, 1321 (2014).
[37]L. Cao, B. Nabet, and J. E. Spanier, Phys. Rev. Lett. **96**, 157402 (2006).
[38]J. Anaya, J. Jimenez, A. Rodriguez, and T. Rodríguez, MRS Proceedings **1627**, (2014).
[39]F. J. Lopez, J. K. Hyun, U. Givan, I. S. Kim, A. L. Holsteen, and L. J. Lauhon, Nano Lett. **12**, 2266 (2012).
[40]J. Anaya, A. Torres, A. Martín-Martín, J. Souto, J. Jiménez, A. Rodríguez, and T. Rodríguez, Appl. Phys. A **113**, 167 (2013).
[41]D. T. Morelli, J. P. Heremans, and G. A. Slack, Phys. Rev. B **66**, 195304 (2002).
[42]R. J. Stoner and H. J. Maris, Phys. Rev. B **48**, 16373 (1993).
[43]J. E. Graebner, S. Jin, G. W. Kammlott, J. A. Herb, and C. F. Gardinier, Nature **359**, 401 (1992).
[44]E. T. Swartz and R. O. Pohl, Rev. Mod. Phys. **61**, 605 (1989).
[45]H. Sun, R. B. Simon, J. W. Pomeroy, D. Francis, F. Faili, D. J. Twitchen, and M. Kuball, Appl. Phys. Lett. **106**, 111906 (2015).